FLASH FLOODS AND PEAK DISCHARGE ESTIMATION

THE SELŠKA SORA RIVER FLASH FLOOD IN SEPTEMBER 2007, W SLOVENIA

Peter Lamovec[1], Krištof Oštir[2], Matjaž Mikoš[3]

ABSTRACT

More and more natural disasters are happening around the world every year: floods, tsunamis, landslides, earthquakes etc. All of them have a common point - they cause large damages and are difficult to be predicted. This paper describes an approach for analysing a flash flood event. The studied area is the Selška Sora River valley in W Slovenia, where a flash flood was caused by the extreme rainfall on 18 September 2007. In the first part of the paper, the determination of flooded areas was done using different data. An extra attention was focused on the satellite images and their applicability to the recognition of the flooded areas. In the second part of the paper, the detected flooded areas were used to compute the selected hydraulic parameters. This study has shown an effective way how to perform a post-flood hydraulic analysis. In the last years, satellite technology has made considerable progress that could significantly improve our ability to assess and predict natural hazards.

Keywords: discharges, flash floods, flooded areas, post-event analysis, rainfall, satellite images

INTRODUCTION

Remote sensing techniques allow us to observe the Earth surface from a distance; no direct contact with the observed part of the Earth is needed. It can be done from the ground (distant standing point), air or space. It is even more useful when wide areas should be observed in a rather short time. The remote sensing images are often the only way to observe some specific areas. Especially in difficult reachable or distant areas (e.g. mountains, deserts) and areas with the infrastructure damaged by a natural disaster, remote sensing is the quickest way to observe these areas. Among them classical ortophoto (aerophotogrammetry), laser scanning (LiDAR) and satellite images can be used. In Slovenia, aerophotogrammetry was already successfully used in the case of the Stože landslide and the wet debris flow in Log pod Mangartom (Kosmatin Fras, 2001). Beside aerophotogrammetry, also satellite images are often used to find out areas damaged by floods (Yonghua et al., 2007; Wang et al., 1995; Liu et al., 2002; Frappart et al., 2006) or landslides (Singhroy et al., 1998; Nichol et al., 2006; Yamaguchi et al., 2003; Komac, 2006). LiDAR (Light Detection And Ranging) is getting an important position in observations of natural hazards and disasters. It makes possible to detect erosion, ground movements and many other geomorphologic structures with vertical accuracy of 10 cm. LiDAR data help us to detect labile ground and define which landslides are still active. Especially the good recognition of the local topographic characteristics is a big advantage of LiDAR (Glenn et al., 2006).

Remote sensing techniques and their applications such as e.g. Proske et al. (2008) have not been often presented at the INTERPRAEVENT congresses; but with a clear increase in the last few years, as confirmed by a search in the intern INTERPRAEVENT database (www.interpraevent.at) using the keywords “remote sensing”.

[1] Peter Lamovec. Institute of Anthropological and Spatial Studies ZRC-SAZU, Novi trg 2, 1000 Ljubljana, Slovenia (e-mail: plamovec@zrc-sazu.si)
[2] Prof. Krištof Oštir. Institute of Anthropological and Spatial Studies ZRC-SAZU, Novi trg 2, 1000 Ljubljana, Slovenia
[3] Prof. Matjaž Mikoš. Faculty of Civil and Geodetic Engineering, University of Ljubljana, Jamova c. 2, 1000 Ljubljana, Slovenia

In the alpine environment, flash floods are more and more frequent events, devastating large areas and causing high economic damages. In many cases, post-event analyses on hydrologic and hydraulic aspects of flash floods are not a trivial task. Different strategies have been developed and applied for real case studies (e.g. Marchi et al., 2009). In this paper we present an application of remote sensing techniques in a real case study, namely of the September 2007 flash floods in W Slovenia.
In September 2007, the weather front that passed over large parts of Slovenia, yielded extreme rainfall that caused several severe flash floods in several parts of Slovenia (Rusjan et al., 2009). During 18 September 2007, in several gauging stations extreme rainfall amounts were measured, e.g. 297mm in 6h, 240mm in 4h, 157 mm in 2h, 95mm in 1h. The post-event analyses were on one hand oriented towards estimation of the return period of the measured rainfall amounts (Rusjan et al., 2009), and on the other hand towards estimation of the peak discharges during the flash floods (Marchi et al., 2009). Since the flash flood hit and devastated mostly the area in the Selška Sora River valley around the town of Železniki, the before mentioned analyses focused to this part in NW Slovenia. Our analysis was oriented on two main topics: firstly to check the efficiency of satellite images to recognize the flooded areas, and secondly to prove that the result of the flood detection is proper to compute relevant hydraulic parameters.

DETERMINATION OF THE FLOODED AREAS IN THE SELŠKA SORA RIVER VALLEY

The area observed and described in this paper is the upper part of the Selška Sora River, i.e. the most populated part of the valley with the three settlements: Železniki, Selca, and Dolenja vas. The determination of the flooded areas was done using different types of data and machine learning techniques.
The satellite SPOT 5 images, digital terrain model (DTM) and the river network were used in this study. The SPOT 5 images contain a spectral information of four bands plus panchromatic. The resolutions and spectral ranges of each band are specified in Table 1. The resolutions of bands from 1 to 4 were increased on 2.5m using the classical pansharpening methods (Švab & Oštir, 2006).

Tab. 1 SPOT 5 satellite spectral bands and resolutions.

Electromagnetic spectrum	Pixel size	Spectral bands
Panchromatic	2.5m	0.48 - 0.71µm
B1: green	10m	0.50 - 0.59µm
B2: red	10m	0.61 - 0.68µm
B3 : near infrared	10m	0.78 - 0.89µm
B4 : mid infrared (MIR)	20m	1.58 - 1.75µm

DTM of two different resolutions was used - DTM 12.5m and DTM 0.5m. The high-resolution digital elevation model (DTM 0.5) was created from the LiDAR measurements for smaller part of the Selška Sora River valley (the area upstream of Železniki). It forced us to make two different classifications - the classification of the whole area using DTM 12.5 and the classification of smaller area using DTM 0.5 (see Fig. 1). DTM is providing necessary information about the terrain: heights, slope and curvature. The river network was used to calculate distances from the main rivers, which were extracted from the vector layer of hydrology in the scale of 1:25,000.
The flooded areas were determined from pre-processed data with machine learning algorithm J48 implemented in the WEKA software. J48 is classifier algorithm for predictive modelling. It was used to find significant patterns from the training data. The patterns are expressed in a form of a decision tree.
The training data consisted of 255 sample points distributed on the treated area of about 2340ha (see Fig. 2). Beside Železniki, two other settlements Selca and Dolenja vas are lying in the area. In order to demonstrate the importance of well-selected sample points two further classifications were carried out – one with larger (400) and another with smaller (49) number of sample points. In a case of higher number of points (400) they were placed also out of the main study area. Many of these points are

redundant. They are lying on higher areas or other areas which are not flooded obviously and do not contribute to better classification.

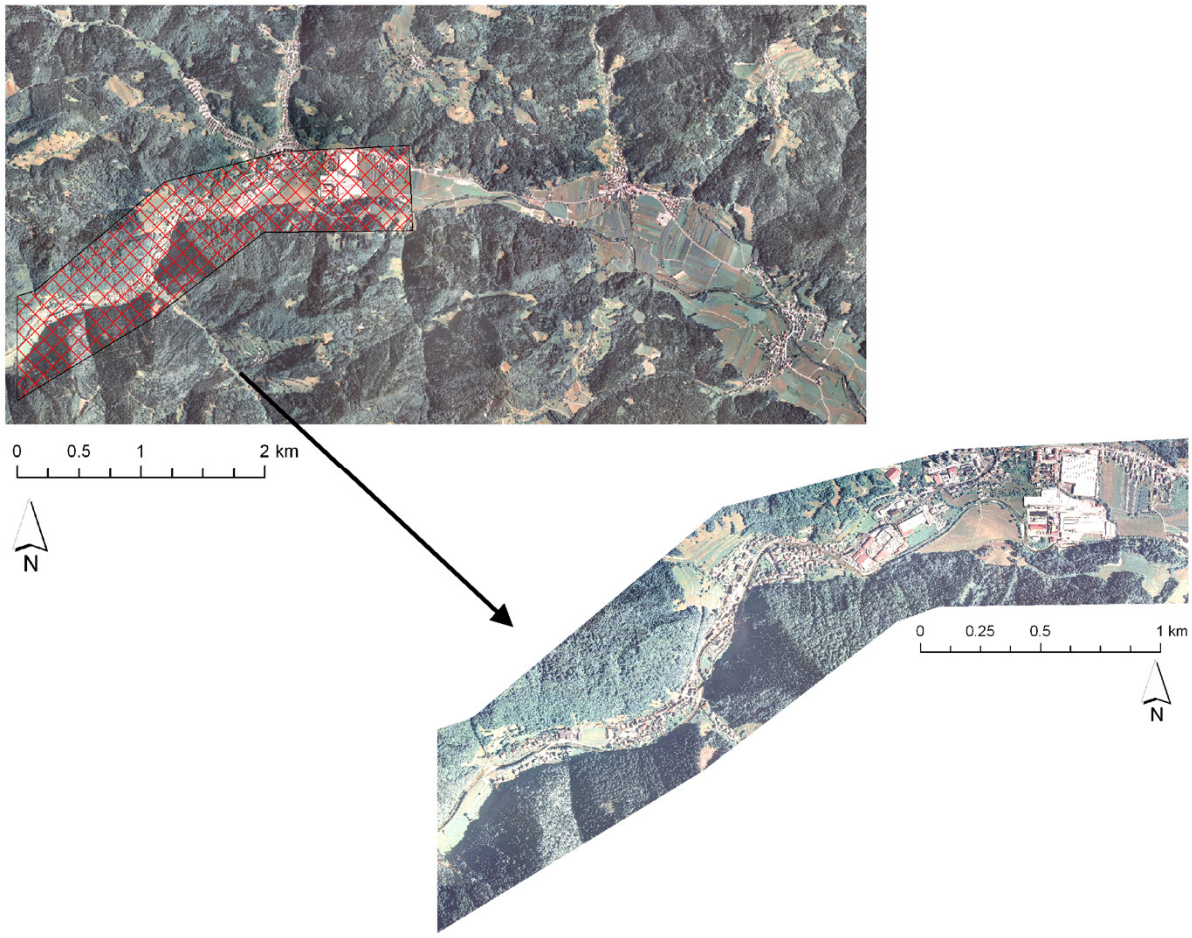

Fig. 1 The study area (above) and its part (below), where LiDAR data exist.

The smaller sample (49 points) was used to test an influence of the ratio between flooded and non-flooded points. The ratio is important because numerically superior attribute values can reduce the importance of those which are less frequent. 24 points were lying on flooded and 25 points on non-flooded areas. In first two samples the number of training points was far lower than number of non-flooded points. The best results were produced using 255 points instead of low balance between flooded and non-flooded points. The area recognized as flooded is too big in other two examples.

The classification on smaller part of the area - the area where the LiDAR data exists (about 254ha in size) - was repeated using machine learning technique. All input data was the same as in the first classification just the relief information (altitude, slope and curvature) was replaced with more accurate data derived from DTM 0.5m. The sample consisted of 146 points (see Fig. 3). The point density was much higher as in the example of whole area. High number of training points was forced on very heterogeneous land cover. Forests, water bodies, agricultural areas and artificial surfaces (buildings, roads) are all mixed on the area. It requires more exactitude in the defining of sampling points. They have to be arranged on all types of land cover. Lower number of training points makes many exchanges between flooded areas and non-flooded agricultural and artificial areas.

The machine learning technique helps to define the attributes that have the most important influence on the classification of flooded areas. The most important attributes are: normalized differential vegetation index (NDVI), bands of multispectral satellite image SPOT B1, B3, B4, distance from water and slope. Distance from water and band B3 are included in the classification with both sample sizes. Other attributes take part on one of them (see Table 2). It is interested that all four bands of multispectral image were active in the classification. Also band B2, which was included into the

classification indirectly by index NDVI. NDVI is calculated from red band (B2) and near infrared band (B3) of multispectral satellite image. Therefore completely all bands of multispectral image take part in the classification process.

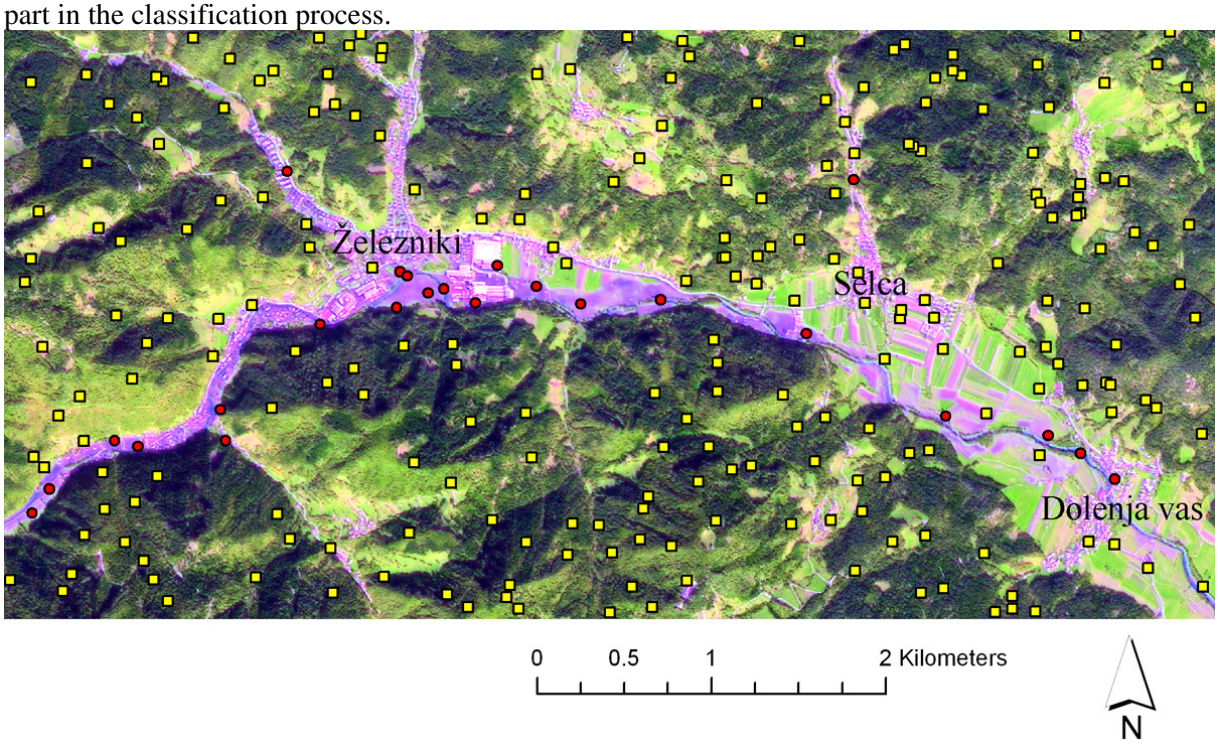

Fig. 2 The training points in the study area: red/circle points are flooded, yellow/square points are lying on non-flooded areas.

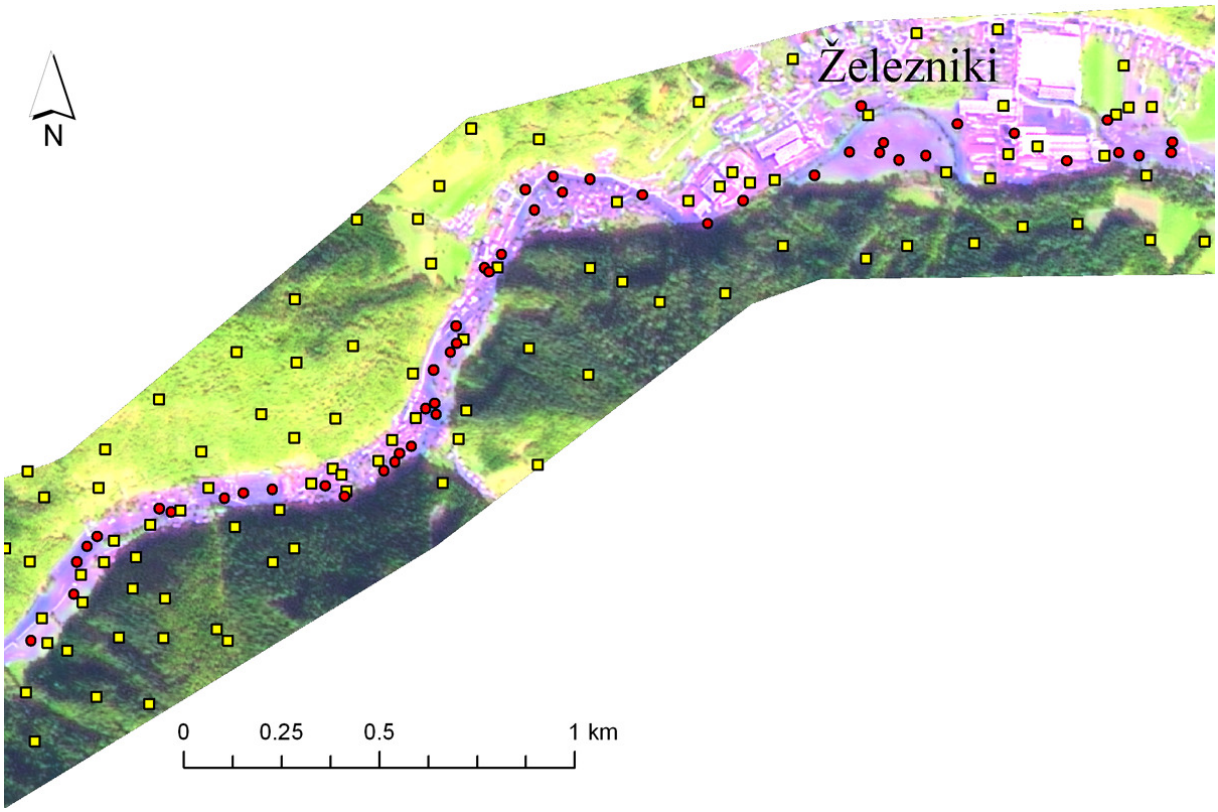

Fig. 3 The training points in the area where LiDAR data exists. Red/circle points present flooded and yellow/square points non-flooded areas.

Tab. 2 Collection of attributes describing sampling points. Symbol ✓ marks the attributes that were used for classification and symbol × marks those that were not.

Attributes:		Classification 1: DTM 12.5m	Classification 2: DTM 0.5m
SPOT image: panchromatic (2.5m)		×	×
SPOT image: multispectral - pansharpening (2.5m)		✓ (bands 3, 4)	✓ (bands 1, 3)
NDVI (Normalized Differenced Vegetation Index)		✓	×
DTM	DTM - Height	×	×
Classification 1: DTM 12.5m	DTM - Slope	×	✓
Classification 2: DTM 0.5m	DTM - Curvature	×	×
Distance from river		✓	✓

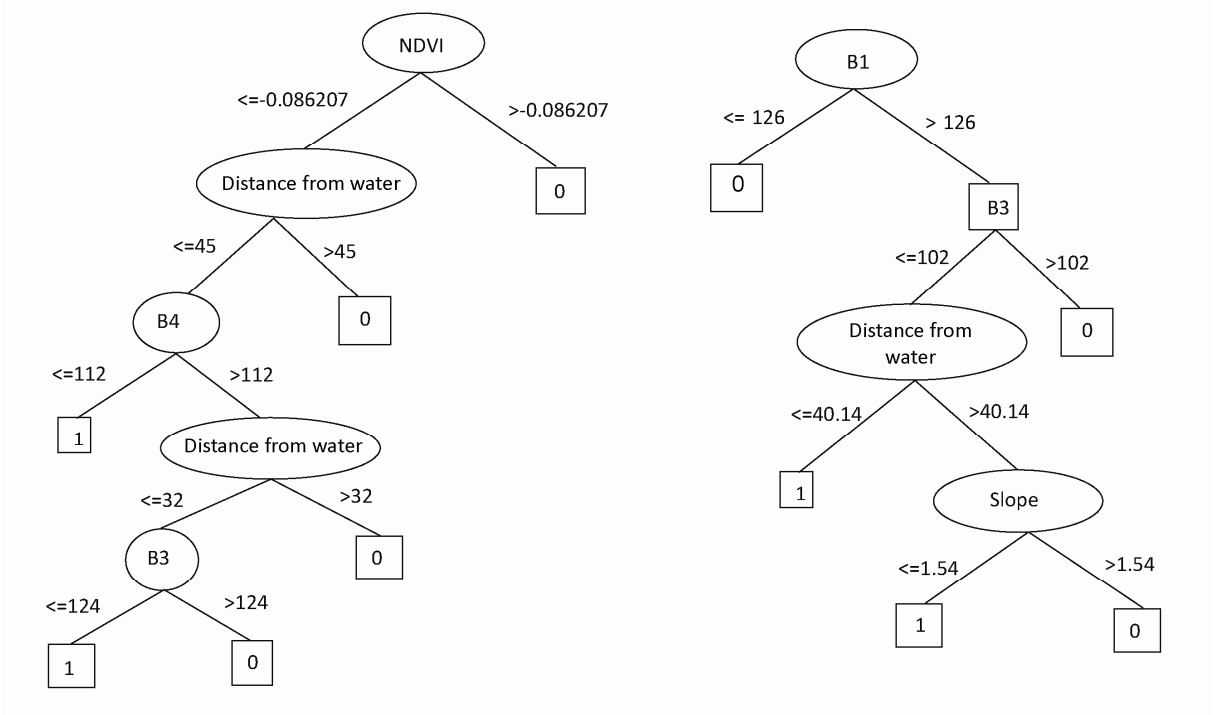

Fig. 4 Decision tree to classify the whole area built from 255 sampling points (left) and the smaller part of the area built from 146 sampling points (right), respectively.

Both decision trees used for classification of bigger and smaller area are shown on Fig. 4. In the case of the first classification where different samples were tested, the best decision tree built from 255 point is shown (see Fig. 4 left). The tree nodes contain important attributes. One attribute is tested in each node - attribute value of each training point is compared with a constant, leaf nodes give a classification that applies to most instances that reach the leaf.

We can see that beside multispectral satellite image also distance from water and slope are present in the decision trees. Their influence is quite expected. The areas far away from the river network are not flooded. If more distant areas were flooded their slope should be lower (the last two nodes on Fig. 4 right). It is normal for the mountain valley where steep slopes limit the flat valley ground and narrow valleys are widen just rarely. The distance from water appears in both classifications while the slope is set just in the second (see Fig. 4 right). It confirms the slope derived from DTM 12.5 (classification 1) is not accurate enough. Its values are changing too much between different measuring points, and this attribute is not significant enough to classify flooded areas. However, slope derived from DTM

0.5 is recognized as one of the crucial attributes for the classification. Therefore DTM 12.5 is useful just for general evaluation of flooded areas, but its accuracy do not allow determination of hydraulic parameters. For this purpose DTM 0.5 is required (see the section on the Determination of hydraulic parameters).

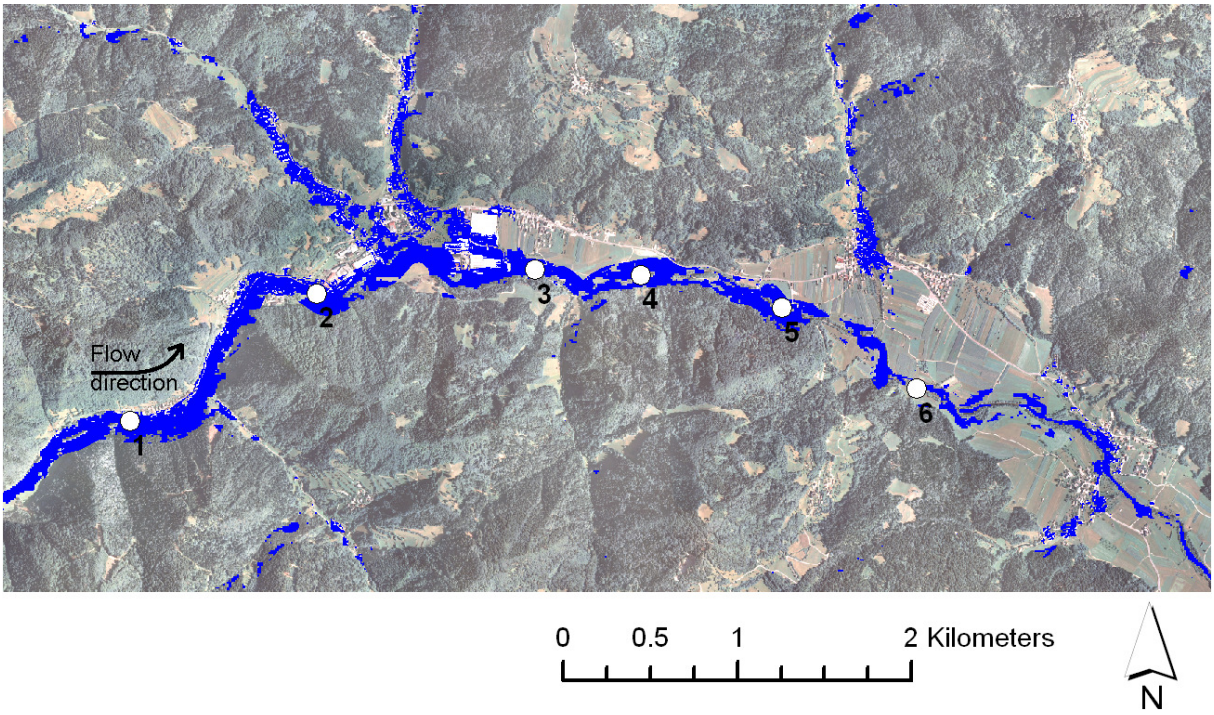

Fig. 5 The recognised flooded areas (blue/dark coloured areas) in the Upper Selška Sora River valley and 6 river valley cross sections used for peak flood discharge estimation (numbered 1 through 6).

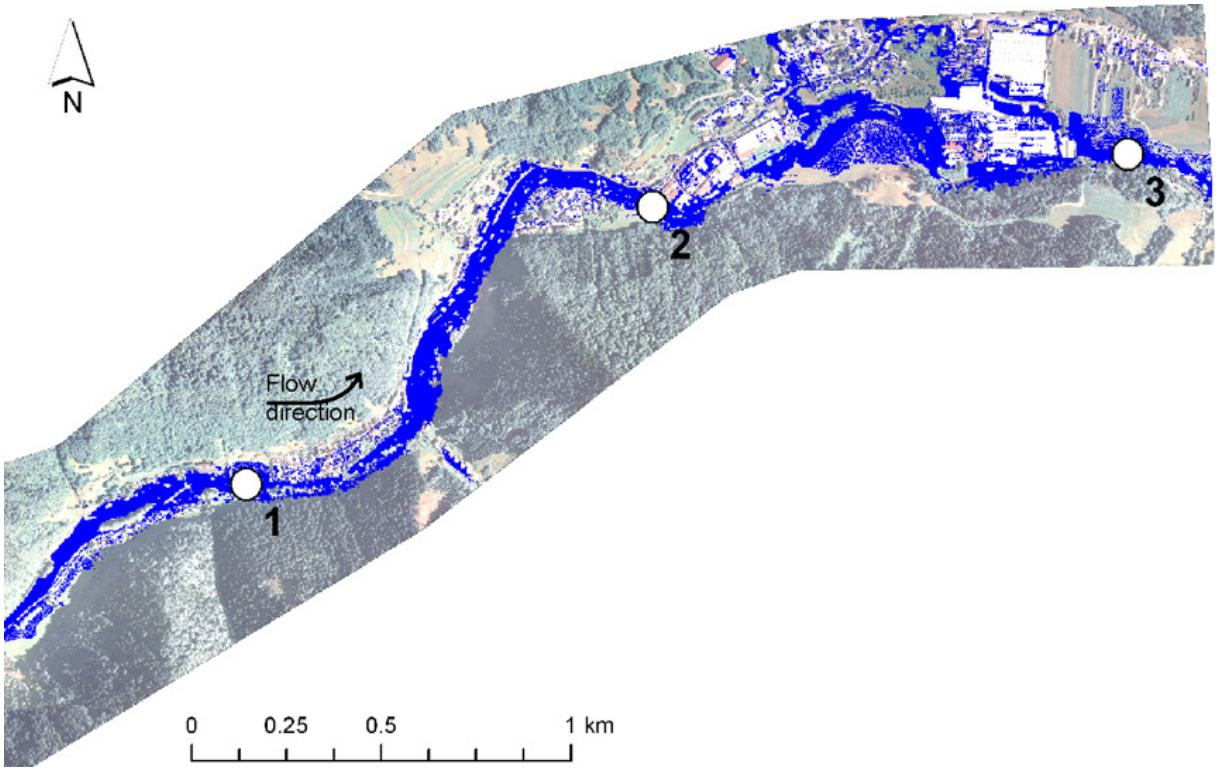

Fig. 6 The recognised flooded areas (blue/dark coloured areas) in the smaller part of Upper Selška Sora River valley and first 3 out of 6 river valley cross sections lying inside of this part of the river stream (# 1 through 3).

The final map was processed in ERDAS IMAGINE. The model built from sampling points was carried on the whole area. At the beginning, all rasters were imported into the model and the conditions of each final class were defined; one raster presents one attribute. The final map of flooded areas is a result of the classification process where each pixel of the raster is classified into the class of flooded or non-flooded areas in a way that all conditions are satisfied (see Figs. 5 and 6). It is seen the flooded areas are not homogeneous. This is a consequence of many areas which were just partly flooded. Trees, some houses and sections of roads extend above the water. Also some higher parts of fields and meadows are also not completely flooded.

DETERMINATION OF HYDRAULIC PARAMETERS

We estimated flood peak discharges during the 18 September 2007 flash flood around the town of Železniki by selecting 6 river valley cross sections. In each of these cross sections, the edge of the flooded area was determined from the maps of the flooded areas (see Figs. 5 and 6). The estimated values of flow parameters in these cross sections are given in Tables 3, 4, and 5.
For hydraulic calculation data about surface height (digital terrain model DTM) are very important. As already described in the section 3, DTM of two different resolutions was used. DTM 12.5m was used for the classification on the whole area (classification 1) and DTM 0.5 was used for smaller area (classification 2). Consequently two different calculations of hydraulic parameters were done, one using DTM 12.5 and another using DTM 0.5. In the latter example hydraulic parameters were calculated just for first 3 out of 6 measuring cross-sections.
The flow cross-sectional area, the wetted perimeter and the Selška Sora River channel longitudinal slope were determined using DEM. Their accuracy depends on accuracy of DTM. It has been proven that DTM 12.5 is unsuitable for determination of relevant hydraulic parameters. The hydraulic parameters derived from DTM 12.5 are not accurate enough for a flood post-event hydraulic analysis. This can be clearly seen from riverbed slope values; its values are varying too much between different cross sections (see Table 3). On the contrary, riverbed slope derived from DTM 0.5 (see Tables 4 and 5) is decreasing regularly along the river.

Tab. 3 The estimated flow parameters in the selected 6 measuring cross-sections of the Selška Sora River. This estimation is based on DTM 12.5.

Parameter in cross section #	#1	#2	#3	#4	#5	#6
Flow cross-sectional area (m^2)	177	144	99	100	146	69
Wetted perimeter (m)	116	88	93	194	137	80
River channel longitudinal slope (-)	0.001	0.009	0.012	0.018	0.004	0.011
Manning roughness coefficient ($m^{-1/3}s$)	0.03	0.07	0.043	0.03	0.03	0.03
Hydraulic radius (m)	1.5	1.6	1.1	0.5	1.1	0.9
Flow velocity (m/s)	1.2	1.9	2.6	2.9	2.1	3.1
Discharge (m^3/s)	205	273	258	285	302	217

Tab. 4 The estimated flow parameters in the first 3 cross-sections out of 6 measuring cross-sections of the Selška Sora River. This estimation is based on DTM 0.5. The river slope values represent the river channel bed slope.

Parameter in cross section #	#1	#2	#3
Flow cross-sectional area (m^2)	132	58	75
Wetted perimeter (m)	104	40	53
River channel longitudinal slope (-)	0.009	0.006	0.003
Manning roughness coefficient ($m^{-1/3}s$)	0.054	0.025	0.035
Hydraulic radius (m)	1.3	1.4	1.4
Flow velocity (m/s)	2.1	3.9	2.0

Discharge (m³/s)	275	226	148

Tab. 5 The estimated flow parameters in the first 3 cross-sections out of 6 measuring cross-sections of the Selška Sora River. This estimation is based on DTM 0.5. The river slope values represent the water surface slope.

Parameter in cross section #	#1	#2	#3
Flow cross-sectional area (m^2)	132	58	75
Wetted perimeter (m)	104	40	53
River channel longitudinal slope (-)	0.005	0.023	0.004
Manning roughness coefficient ($m^{-1/3}s$)	0.040	0.038	0.035
Hydraulic radius (m)	1.3	1.4	1.4
Flow velocity (m/s)	2.0	5.0	2.3
Discharge (m³/s)	260	292	171

It seems its values describe the valley bottom and the river channel slope much more correctly. Two different values of slope were used for calculation of hydraulic parameters. Slope values present channel bed slope in Table 4, and water surface slope in Table 5. Water surface slope has to be taken into account in a case of flood post-event hydraulic analysis. It was defined as linear regression between three points on distance 60m (see Fig. 7). Additionally, the average valley slope was estimated to 0.01.

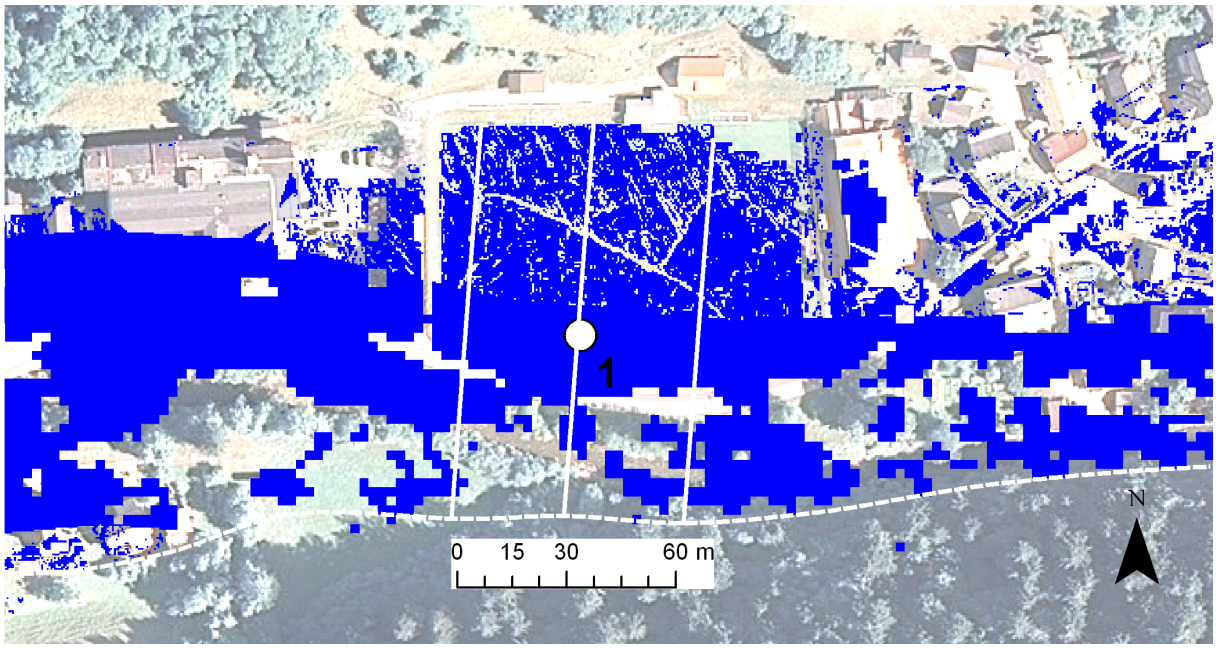

Fig. 7 Water surface slope definition on the measuring point 1. The slope was defined as a linear regression between three cross sectional lines on distance 60m. The recognized flooded area (blue/dark coloured areas) is not homogeneous because some interruptions are happening (tress, houses...). Therefore DTM was used to define the edge of flooded area. The edge on the south side of the river is marked by dashed line.

The Manning roughness coefficients were determined from our past experiences with hydraulic modelling taking field conditions into account, and were not measured in any way. The selected values for the Manning coefficient for a riverbed with deep flooding water (~0.035s.$m^{-1/3}$) is lower from the ones selected for shallow overflow in a flooded areas (~0.030s.$m^{-1/3}$ to ~0.070s.$m^{-1/3}$) where also many obstacles (tress, houses) are present. The final values of the Manning coefficient of a river valley cross section are compound values of the before mentioned values for the riverbed and the flooded area.

The different Manning coefficient values were tested to get the estimated discharge of ~300m^3/s that is believed to be a close approximation to the real peak discharge (Rusjan et al., 2009). On one hand, the Manning coefficient was defined considering the wetted perimeter (see Table 4), and on the other hand, its value was defined considering the cross-sectional area instead of the wetted perimeter (see Table 5); the latter approach being a more accurate approximation from a hydraulic point of view.
The flow velocities and flood discharges in the river valley cross sections were determined using the Manning-Strickler equation. The riverbed longitudinal slope is the weakest member in the first estimation of hydraulic parameters based on DTM 12.5 (see Table 3). Their values should not be much different from the general river valley slope, which is 0.01. Similarly can be said about the hydraulic radius and their values also vary a lot between measuring sites, and are also rather low, as concluded from our past flood experiences. As a consequence, flow velocities are rather low for a flash flood, and peak discharges are therefore rather underestimated. For comparison, we may quote estimated peak discharges from extrapolation of measuring data from the gauging station in the Town of Železniki, and these were (Rusjan et al., 2009): below 300m^3/s upstream of Železniki (cross sections 1 & 2), and ~ 300m^3/s downstream of Železniki (cross sections from 3 to 6).
A better result is obtained using parameters derived from DTM 0.5 (see Table 4). DTM 0.5 gave much better information on relief and channel bottom in the cross sections specially. More correctness in definition of wetted perimeter and flow cross-sectional area contributed to more accuracy in hydraulic radius, flow velocity and finally discharge. However, there are still some problems with river channel longitudinal slope and the Manning roughness coefficient. Especially slope is varying too much. Therefore some additional improvements were done in Table 5. Channel bed slope in Table 4 is replaced with water surface slope in Table 5, and the Manning roughness coefficient is defined considering cross-sectional area instead of wetted perimeter as in Table 4. These modifications ensure quite good approximation of relevant hydraulic parameters to their real field values in the cross section 2 (Rusjan et al., 2009). The discharge values seem to be low in the cross section 1 and 3. It is a consequence of a gentle water surface slope compared to the valley slope. Their estimated values of 0.005 in the cross section 3 and of 0.004 in the cross section 4 are rather small. If they were closer to the average valley slope of 0.01, also the discharges would be higher. Furthermore, the best results are in the cross section 2 where the most water was caught into the riverbed and where the overflow was limited. Therefore the wetted perimeter is smaller, the flow velocity is higher and the discharge is increased. In the cross section 1 and 3 overflow was happening. The flow velocity is too low and the discharge is underestimated. It is a consequence of water stagnancy/overflowing on these areas.

CONCLUSIONS

The meteorological and hydrological data represent an important part of data to understand phenomenon of floods. Data about precipitation, discharges etc. enables the analyses of flood events. Adequate analyses are necessary to make sanitation of flooded areas correctly to prevent the area before another disaster and to predict floods and to warn habitants before another danger. Effective modelling has to include topographic characteristics of the area. Many topographic characteristics are described by digital terrain model. It helps to predict the response of the area on specific meteorological and hydrological situation. The importance of such analyses was shown by Rusjan et al. (2009) before.
This article puts out relatively effective way to define hydraulic parameters. At first the flooded surface has to be defined exactly. It was done by using satellite images, DTM and the river network. This data were analysed using machine learning technique. It is a very practical way to classify flooded areas when a lot of data and a large area have to be analyzed. Exactly defined flooded area allows extraction of the edge of the floods and furthermore the definition of hydraulic parameters. The study shows that the combination of satellite images and DTM assures the calculation of hydraulic parameters. It focuses also on the necessary resolutions of data. While a resolution of satellite images 2.5m was sufficient, a resolution of DTM was discussed more. The determination of hydraulic parameters on DTM with a resolution of 12.5m and 0.5m was done. The analysis showed that DEM 12.5 do not allow estimating hydraulic parameters with an acceptable accuracy. Channel bottom in some cross sections cannot be easily recognised from DTM 12.5. Contrarily, the hydraulic

parameters derived from DTM 0.5 are more reliable and more comparable to the measuring data from the gauging station in the town of Železniki (Rusjan et al., 2009). However, DEM of a sufficient resolution was just one of the conditions to calculate hydraulic parameters successfully – the correct recognition of the flooded areas had to be done before.

REFERENCES

Frappart F., Do Minh K., L'Hermitte J., Cazenave A., Ramillien G., Le Toan T., Mognard-Campbell N. (2006). Water volume change in the lower Mekong from satellite altimetry and imagery data. Geophysical Journal International 167(2): 570-584.

Glenn N.F., Streutker D.R., Chadwick D.J., Glenn D.T., Dorsch S.J. (2006). Analysis of lidar-derived topographic information for characterizing and differentiating landslide morphology and activity. Geomorphology 73(1-2): 131-148.

Komac M. (2006). A landslide susceptibility model using the Analytical Hierarchy Process method and multivariate statistics in perialpine Slovenia. Geomorphology 74(1-4): 17-28.

Kosmatin Fras M. (2001). Vloga fotogrametrije in prostorskih podatkov pri dokumentiranju naravnih katastrof - primer plazu pod Mangartom (The role of photogrammetry and spatial data in documenting natural disasters – a case study of the landslide below Mangart). Geodetski vestnik 45(1&2): 62-71. (in Slovenian)

Liu Z., Huang F., Li L., Wan E. (2002). Dynamic monitoring and damage evaluation of flood in north-west Jilin with remote sensing. International Journal of Remote Sensing 23(18): 3669-3679.

Marchi L., Borga M., Preciso E., Sangati M., Gaume E., Bain V., Delrieu G., Bonnifait L., Pogačnik N. (2009). Comprehensive post-event survey of a flash flood in Western Slovenia: observation strategy and lessons learned. Hydrological Processes 23(26): 3761–3770.

Nichol J., Wong M.S., Shaker A. (2006). Application of high-resolution satellite images to detailed landslide hazard assessment. Geomorphology 76(1-2): 68-75.

Proske H., Granica K., Hirschmugl M., Wurm M. (2008). Landslide detection and susceptibility mapping using innovative remote sensing data sources. INTERPRAEVENT 2008, Conference proceedings, Vol. 2, 219-229.

Rusjan S., Kobold M., Mikoš M. (2009). Characteristics of the extreme rainfall event and consequent flash floods in W Slovenia in September 2007. Natural Hazards and Earth System Sciences 9(3): 947-956.

Singhroy V., Mattar K.E., Gray A.L. (1998). Landslide characterisation in Canada using interferometric SAR and combined SAR and TM images. Advances in Space Research 21: 465-476.

Švab A., Oštir K. (2006). High-resolution image fusion: methods to preserve spectral and spatial resolution. Photogramm. eng. remote sensing 72(5): 565-572.

Wang Y., Koopmans B.N., Pohl C. (1995). The 1995 Flood in the Netherlands Monitored from Space - a Multisensor Approach. International Journal of Remote Sensing 16(15): 2735-2739.

Yamaguchi Y., Tanaka S., Odajima T., Kamai T., Tsuchida S. (2003). Detection of a landslide movement as geometric misregistration in image matching of SPOT - HRV - data of two different dates. International Journal of Remote Sensing 24(18): 3523-3534.

Yonghua S., Xiaojuan L., Huili G., Wenji Z., Zhaoning G. (2007). A study on optical and SAR data fusion for extracting flooded area. Geoscience and Remote Sensing Symposium. IEEE International. 3086-3089.